Active Control of Resonant MHD Modes in RFX-mod

L. Grando, G. Manduchi, L. Marrelli, G. Marchiori, R. Paccagnella, P. Piovesan, L. Piron, A. Soppelsa, G. Spizzo, P. Zanca

Consorzio RFX, Associazione EURATOM-ENEA sulla Fusione, Corso Stati Uniti, 4, 35127-Padova, Italy

e-mail contact of main author: lionello.marrelli@igi.cnr.it

Abstract. Thanks to the development of a new control algorithm, named clean mode control (CMC), the control of the effects of m=1 resistive-kink and tearing modes (TMs) on the reversed field pinch RFX-mod has significantly improved, compared to previous virtual shell (VS) operations. The CMC algorithm is based on the real-time removal of a systematic error affecting magnetic measurements due to the aliasing of the sideband harmonics produced by the active coils. CMC brings several advantages over VS: the non axi-symmetric deformation of the last closed magnetic surface decreases; wall unlocking of TMs is systematically obtained; TMs phase locking is weakened, the plasma wall interaction pattern moves during each discharge and it is more toroidally distributed, assuming a helical pattern.

1) Introduction

The active control of magnetic field perturbations is very important for fusion research: in fact, since a close fitting passive shell cannot be used for a steady state reactor, the development of methods for actively preventing the growth of MHD instabilities and to correct error fields are mandatory.
The reversed field pinch (RFP) device RFX-mod (R/a=2.00 m/0.459 m) is equipped with an actively controlled magnetic boundary and allows conducting experimental investigations on these issues. The RFP configuration is characterized by the presence of an infinite number of resonant surfaces that may lead to the excitation of m=1 resonant resistive modes [1]. These modes, whose radial profiles span the whole radius, provide the means to drive the currents required by the magnetic configuration (dynamo effect [2]) and they are present even with a perfectly conducting wall located at the plasma edge. The dynamo process can be either "laminar", i.e. based on a single mode (Single Helicity, SH), or "turbulent", when many modes are simultaneously present (Multiple Helicity, MH). Pure SH is not observed in experiments yet, but quasi single helicity states (QSH) occur, where a single mode dominates over a residual level of secondary ones [3]. The internal resonant resistive modes, which are defined tearing modes (TM), significantly affect both the core, where they determine the level of particle and energy transport, and the edge, where they cause non axi-symmetric deformations of the shape of the last closed magnetic surface. The reduction of these deformations is a crucial issue for reducing plasma wall interaction, which in Multiple Helicity RFPs is affected by the phase-locking and wall-locking phenomena [4],.
Tearing Modes dynamics is strongly influenced by the properties of the magnetic boundary, as shown by nonlinear 3D MHD simulations where a careful adjustment of a feedback law is shown to induce transitions to a SH state [5]. This relation can be investigated by means of the highly flexible RFX-mod control system. The plasma is surrounded by a thin copper shell (the effective shell time, including also the shell support structure is τ_b=124ms) covered by 48x4 saddle coils with independent power supplies. Radial field sensor loops of the same size as the active coils are located inside the shell. In the simplest control scheme, dubbed Virtual Shell (VS) [6], the flux through each sensor loop is controlled by the corresponding active coil. Compared to passive operations, the VS scheme allowed a considerable improvement of plasma performances: Resistive Wall Modes were stabilized [7] and plasma wall interaction due to wall locked TMs was mitigated [8]. Careful analysis (summarized in paragraph 1)

revealed that the action of the VS scheme on the edge amplitude of the TMs is limited by a systematic error: the measured magnetic field harmonics includes the aliasing of the high poloidal and toroidal mode number sidebands produced by the discrete coils grid. Such aliasing effect has been identified and corrected in real time [9]: after the first successful experiments of a Mode Control approach using clean Fourier harmonics as feedback variables [10], extensive optimization campaigns have been performed. The main findings of the still ongoing optimization campaign are summarized in paragraph 3: systematic wall unlocking and reduction of non axisimmetric deformation due to m=1 TMs is obtained. CMC allowed exploring high current regimes, where QSH occur more often: in such conditions the phase dynamics of the dominant mode depend on the control system (paragraph 4). Plasma wall interaction is reduced in CMC (paragraph 5).

2) Limitations of the Virtual Shell scheme: the aliasing of sidebands

In the Virtual Shell scheme the target of the control system is to keep the measurement of each radial field sensor coil $b_r^{i,j}$ (i=1..48,j=1..4) as close to zero as possible. In this scheme, the current flowing into each control coil is determined by a feedback law with a Proportional Integral approach. The action of the control system is different on the RWMs and the TMs. This can be observed because TMs and RWMs are m=1 modes characterized by different toroidal numbers. TMs are resonant inside the plasma (i.e. n<-6 in RFX-mod), while RWM are non resonant both internally (-1<=n<=-6) and externally (n>1) [11].
The Fourier spectrum (averaged between 60 and 120ms for a set of 800kA discharges) of the toroidal component of the MHD instabilities for an ensemble of VS discharges is given in Figure 1a. The spectrum is dominated by modes with n<=-7, corresponding to TMs, while the amplitude of the spectrum for the RWM helicities is negligible. Note that the n=-7 amplitude dispersion is higher, due to the tendency of developing intermittent QSH states. Figure 1b shows the spectrum of the radial field produced by the saddle coils. This is computed by means of a cylindrical model using the measured currents flowing into the saddle coils [9]. While the external action in the RWM branch is quite low (theory predicts, in fact, that RWM modes are stabilized [11]), a significant amount of external radial field is supplied in the TM branch (n<=-7). The overall effect is that the discrete Fourier transform of the radial field measured by sensors (black circles in Figure 1d)) is very low. The VS scheme successfully cancels the *measurements* of the radial fields. In fact, the applied radial field is opposed to the radial field generated by the plasma: this is proved by Figure 1c) which shows the phase difference between the toroidal field pertubations and the applied radial field. Such phase difference is almost π/2. Assuming that the toroidal component is mainly due to the TMs, the TM radial field harmonics are -π/2 phase shifted with respect to the toroidal field component, therefore the applied radial field is opposite to the plasma radial field.
Cancellation of measurements, i.e. of the DFT harmonics, does not necessarily imply that the

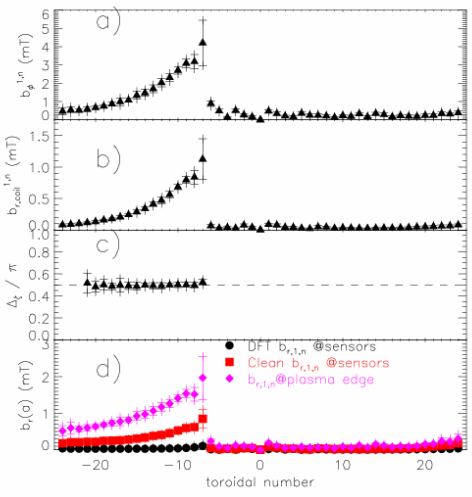

Figure 1) *a) spectrum of toroidal magnetic pertubations ; b) saddle coils produced radial field spectrum; c) phase difference between spectra a) and b); d) radial field spectrum (black circles: DFT, red squares sideband cleaned, magenta diamonds, field at plasma edge)*.

Fourier harmonics are cancelled. Square symbols in Figure 1d) represent, the "clean" Fourier spectrum, which is significantly different from zero.
The difference between DFT and Fourier harmonics is a consequence of the well known Nyquist's sampling theorem, which states that the DFT harmonics (i.e. the Fourier coefficients of a discrete periodic sequence) correspond to Fourier harmonics only if the spectrum is contained within the Nyquist frequency. If this condition is violated the *aliasing* phenomenon occurs: i.e. Fourier harmonics with high toroidal number appear in the DFT spectrum at a lower toroidal number, which depends on the number of sensors. While the toroidal numbers of the RFX-mod spectrum of MHD instabilities falls within the Nyquist interval, the same does not hold for the field produced by the saddle coils. It has been in fact shown that a net of MxN saddle coils covering a torus can produce radial fields with helicities up to m=M/2 and |n| up to N/2 together with an infinite number of *sideband harmonics* [11,9]. The sideband harmonics depend on the number and on the geometry of the saddle coils and cannot be eliminated. Sidebands can be measured if the number of sensors is much greater than the number of active coils. In the VS scheme, the number of sensors corresponds to the number of active coils and therefore the still occurring aliasing of sidebands does not appear in the DFT spectrum. For example, if the system of 48x4 RFX-mod coils is generating an m=1, n=-7 radial field, all the sideband harmonics, e.g. the m=1,n=-55, m=1,n=41, etc., will all be aliased into the m=1,n=-7 DFT coefficient. The aliasing of sidebands was considered in [11] but found not relevant for the stabilization of Resistive Wall modes.
A cleaning algorithm has been developed to remove the aliasing of sidebands from the measurements, under the reasonable assumption that only the saddle coils produce harmonics beyond the Nyquist frequency [9]. The residual level of radial field in the TM harmonics (square symbols in Figure 1d) is therefore significantly higher than what would be inferred from DFT coefficients (open circles in Figure 1d). Finally, Figure 1d) shows another important source of systematic error, which is due to the radial distance between the sensor coils (located at r_c=0.507): magenta diamonds represent the radial field extrapolated at the plasma edge, determined by the solution of the standard vacuum equation for the magnetic field in cylindrical geometry, using as boundary conditions the clean Fourier harmonics of the radial and of the toroidal field. The radial field at the plasma edge is significantly higher than the field at the sensor radius. Therefore, even a perfect cancellation of the radial field at the sensors does not imply that the field is zero at the plasma edge. The cleaning and the extrapolation algorithms have then been implemented in the real-time, requiring a significant upgrade of the control system [12].

3) Clean Mode Control optimization

Since the discovery of the systematic error due to the aliasing of sidebands, most experiments have been performed with a mode control scheme. A feedback law is defined on the Clean Fourier harmonics, instead of the DFT ones, extrapolated to the plasma edge. In this scheme, dubbed "Clean Mode Control", the current harmonic $I^{coil}_{m,n}(t)$ reference to be produced by the saddle coils is given through a proportional integral derivative (PID) feedback law

$$I^{coil}_{m,n}(t) = -K_P e_{m,n}(t) - K_I \int_0^t dt\, e_{m,n}(t) - K_D \frac{d}{dt} \Im\left(e_{m,n}(t), f_{cut}\right) \quad \text{Eq 1)}$$

The error signal $e_{m,n}(t)$ is the complex amplitude of the clean Fourier harmonic. Coefficients $K_P^{m,n}$, $K_I^{m,n}$ and $K_D^{m,n}$ are real constants representing the proportional, integral and derivative gains, respectively, which may be different for every mode. The derivative action is performed on a one pole low pass filtered version of the signal ($\Im\left(e_{m,n}(t), f_{cut}\right)$), with cut-off frequency f_{cut} of 300 Hz. The actual reference value for the saddle coils are obtained by

performing a real time inverse discrete Fourier transform of the modal references defined in Eq. 1 at each control cycle.

An initial design of the mode controller with a Proportional Derivative (PD) approach was carried out on the basis of a simple model of the passive conductors (shell and supporting mechanical structure) [10]. It was found that the choice of gains had important consequences not only on the edge amplitude but also on the TM phase. Single mode gain scans showed, in fact, that below a critical gain the mode phase was wall locked while for higher values of the proportional gain, the mode phase was no longer stationary but rotated up to 100 Hz. This behaviour is reproduced by a simplified torque balance model [9], based on Newcomb equation solution for the TM radial profile and the thin shell dispersion relation.

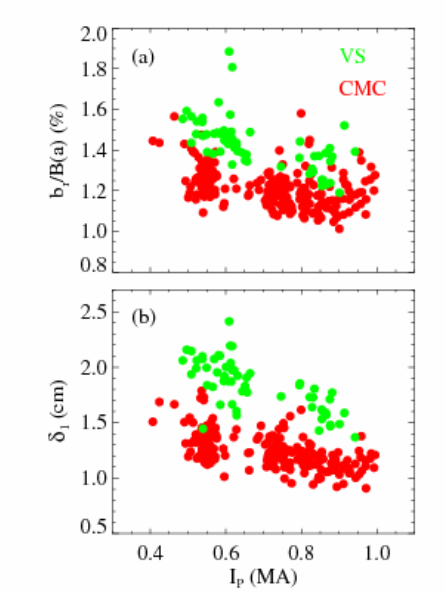

Figure 2) *a) RMS of the m=1 edge radial field, normalized to the poloidal field. b)*. δ_1 *vs plasma current for CMC (red cross) and VS (green diamonds)*

After gain optimization, the first important result of CMC is that lower values of the edge radial field are obtained comapred to VS, as shown in Figure 2a where the square root of the quadratic sum of clean radial field harmonics at the plasma edge is plotted as a function of the plasma current. The reduced b^r leads to the decrease of the localized non axi-symmetric displacement of the last closed magnetic surface δ_1, as shown in Figure 2b.

A second important result of CMC control is that wall unlocking of the TM phases is systematically obtained. The rotation frequency is not constant and may even change sign during the discharge. A statistical description of the phase variation is obtained by determining the median of the instantaneous rotation frequency, estimated by linear fitting the TM phase on a 5 ms time window. Figure 3a shows that in VS the median frequencies are always very close to zero for all modes, while in the CMC a significant spread of the distribution of median frequencies is observed. It is interesting to observe that the medians of the frequencies are correlated (Figure 3b) suggesting that phase locking still occur.

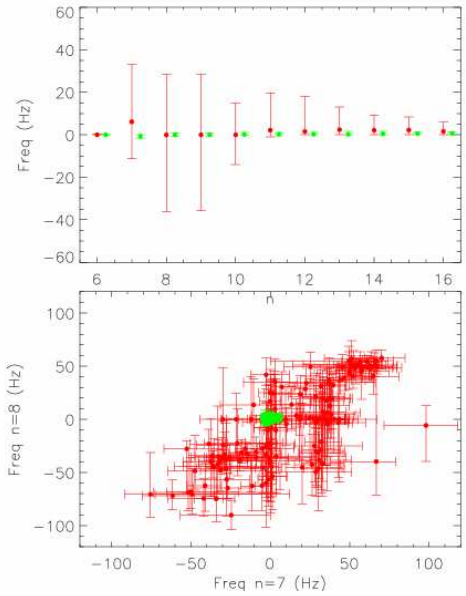

Figure 3) *a) rotation frequencies for VS (green) and CMC (red); b) correlation between the medians of m=1,n=-7 and m=1,n=-8 TMs*

More precisely, phase locking between different modes can be quantified by analyzing the locking strength indicator [13] which represents, on a scale from 0 to 1, the degree of constructive interference of the ensemble of TMs: in this case modes with n=-8,..,n=-23 are considered. In VS the phase locking is almost always very close to 1, while in CMC intermittent reductions of phase locking frequently occur. A statistical comparison between CMC and VS is obtained by averaging

the locking strength over 1ms windows during the flat top phases of the CMC and VS ensembles. The distribution functions (shown in Figure 4a) are peaked at 1 but lower locking strength values are significantly more frequent in CMC than in VS.

Even though TM phases are often phase locked, the toroidal angle of the position of constructive interference is never stationary in CMC discharge. A quantitative comparison of this behaviour in CMC and in VS cannot be directly based on the standard deviation of the locking angles time series, because it is not a well defined quantity for directional data. It is customary to represent angles with unit vectors: this allows, for a given ensembles of angles, to define an average vector (which is less or equal to unit length), which contains information both on the average and on the dispersion of the dataset. In fact, while the angle of this vector represents the average angle of the distribution, its magnitude represent the dispersion. A value of 1 indicates that all angles are identical, while a value of 0 is consistent with a uniform distribution. For each discharge in the dataset, the distribution of the locking position toroidal angles, sampled in 1 ms time intervals during the flat top is considered and the average vector is computed. We define its magnitude as the dispersion coefficient C_l. If C_l is 1, the locking position is stationary in time. On the contrary, lower C_l values indicate that the locking position changes during the discharge.

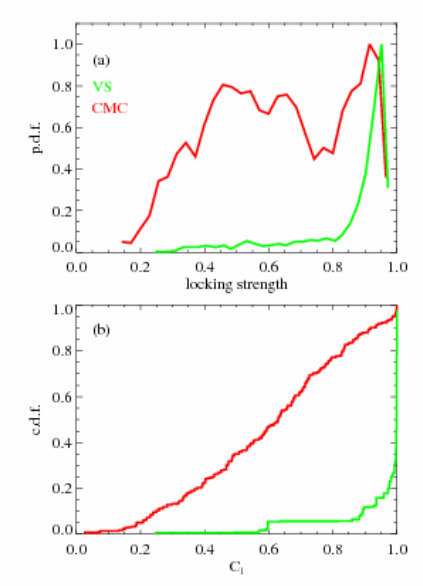

Figure 4) a) *Probability distribution function of the locking strength computed in 1 ms time windows for the two sets of VS and CMC discharges; b) Cumulative distribution of the C_l coefficient*

The cumulative distribution of C_l for VS and CMS discharges is shown in Figure 4b). The coverage coefficient C_l for VS discharges is always greater than 0.6 indicating that the locking position is almost always stationary while in CMC discharges the locking position very often varies during discharges.

3.1) Experiments with Complex gains

Experiments have been attempted aiming at reducing the phase locking among modes, in order to further decrease the maximum value of the non axisymmetric distortion δ_1. The Clean Mode Control feedback law was obtained by modifying eq 1 as follows.

$$I_{m,n}^{coil}(t) = -K_{P,m,n}\exp(i\varphi_{m,n})e_{r,m,n}(t)$$

No derivative or integral gains were considered and the proportional gain is allowed to assume complex values: $K_{P,m,n}$, and $\phi_{m,n}$ are the amplitude and the phase of the complex proportional gain. The phase $\phi_{m,n}$ therefore represents the phase difference between the *measured* field harmonic and the *applied* field harmonic. It is found that the direction of the mode rotation is reproducibly determined by the sign of the phase $\phi_{m,n}$,. The value of the phase does not influence the rotation frequency, at least for the chosen value of

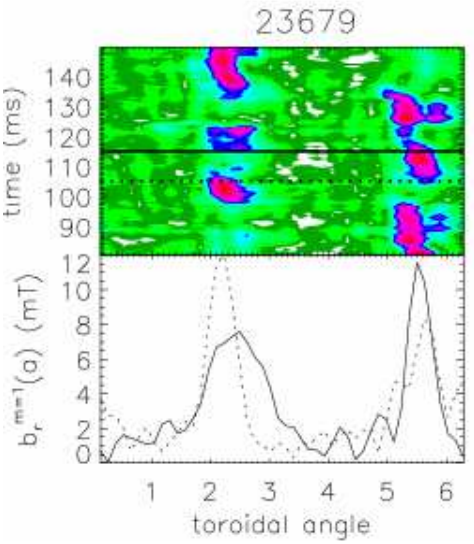

Figure 5) *time evolution of the m=1 deformation of the edge radial field*

$K_{P,1,-7}$. It is also possible to determine simultaneously the sign of the rotation for several modes: complex gains of opposite sign have been set on the dominant modes for n≤-8, excluding the innermost resonant. While the direction of the phase rotation actually follows the alternate pattern, no significant reduction of the maximum displacement due to the m=1 modes is observed. The deformation of the last closed magnetic surface tends to show a secondary local maximum of similar amplitude, as shown in Figure 5. In time, the maximum of the deformation jumps between these two locations. Consequently, complex gains were set only on low amplitude high n (n<-12) tearing modes, while different proportional and proportional-derivative gains were set for dominant modes, in order to vary the modes' phase locking.

4) Dynamics of Quasi Single Helicity states

Quasi Single Helicity states may develop both in CMC and in VS discharges: in particular it appears that they occur more frequently at high plasma current. A more quantitative statement is based on the QSH persistence indicator [14], defined as the ratio between the total time (even in non consecutive intervals) during which a QSH is present and the current flat-top period. The QSH frequency is similar in CMC and in VS, at similar currents. The exploration of higher current regimes (I_p > 0.8MA) is not possible in VS, due to the TMs wall locking and subsequent plasma wall interaction. Experiments up to 1.1 MA have been performed with a modified version of the VS algorithm, but with a significantly low QSH persistence [10].

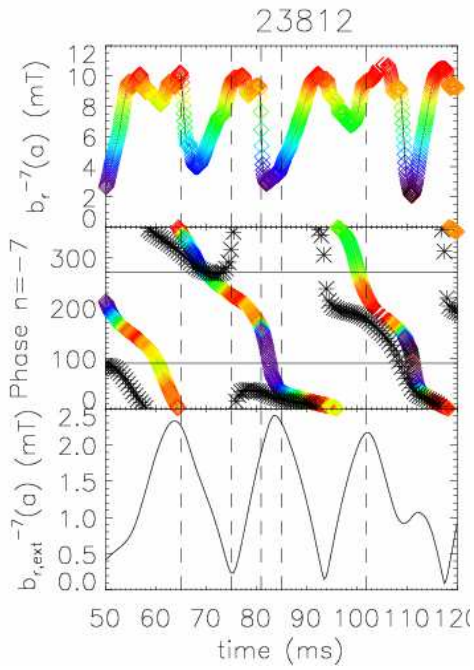

Figure 6). *a) dominant mode edge radial field amplitude, b) mode phase (the color encodes the mode amplitude) and externally applied field phase (*); c) m=1,n=-7 penetrated radial field produced by the saddle coils.*

The presently observed dynamics of the dominant mode in CMC is relatively fast and rather high values of the m=1, n=-7 edge radial field are measured (on average 2%-3% of the poloidal field at the edge during the flat top), as shown in Figure 6a. Panel b) of Figure 6 shows the phase dynamics of the QSH which is characterized by a reproducible behavior. The phase velocity is, in fact, significantly reduced during the growth of the mode amplitude and it accelerates again when the mode crashes. Moreover, in the subsequent growth cycle, the phase is approximately at 180 degrees compared to the previous one. Such a behavior is determined by the control system: in fact, the saddle coils are located outside the mechanical structure and the shell. Therefore, once the TM amplitude drastically reduces, the penetrated field (shown in Figure 6c) cannot decrease as fast, due the shell penetration time scale. Such a field acts as a seed and the m=1,n=-7 TM phase aligns to it (panel b). During this aligned phase, the control system reacts and the penetrated field decreases (panel c) as the feedback law aims at opposing the radial field produced by the plasma. This behavior is qualitatively reproduced by the torque balance model, described in [9], provided that the experimentally estimated amplitude of the mode at the resonant radius is used. A systematic investigation of the effect of the control system on the TM amplitude is still in progress in order to seek conditions for avoiding the crash of Quasi Single Helicity.

5) Effects of TM control on Plasma-Wall Interaction

The successful systematic wall unlocking drastically leads to a more uniform vessel temperature increase, as measured by arrays of thermal sensors [9] in CMC discharges. Time resolved information on plasma wall interaction can be obtained by analyzing total radiation measurements obtained by the RFX-mod bolometric tomography. Toroidally localized, highly emissive spots have been observed in the past in the RFX experiment [15] in the locked mode region, and correspond to cold regions of high neutral and impurity (mainly Carbon and Oxygen) influx: they were responsible for resistivity increase and abnormal discharge termination [16]. A suitable indicator of the toroidal localization of total radiation is the spatial R.M.S. of the poloidal integral of the emissivity map ("linear" emitted power density, unit MW m^{-1})

$$\Pi_{rad}(\phi) = \int_0^{2\pi} d\theta \int_0^a r\, dr\, \varepsilon(r,\theta,\phi)$$

where ε is the bolometric emissivity and *a* the minor radius. Since the RFX-mod tomography reconstructs an emissivity map at fixed toroidal location ϕ_{tomo}, it is possible to measure only one toroidal point at a given time. Assuming that the bolometric emissivity pattern remains constant around the location of the maximum deformation due to the locked TMs, it is possible to transform time into toroidal angle: therefore plotting Π_{rad} as a function of ϕ_{tomo}-ϕ_{lock}(t) (ϕ_{tomo} is the toroidal location of the tomography, ϕ_{lock}(t) locking angle) we can reconstruct the toroidal distribution of the radiated power. In CMC total radiation is toroidally more uniform, compared to VS (Figure 7).

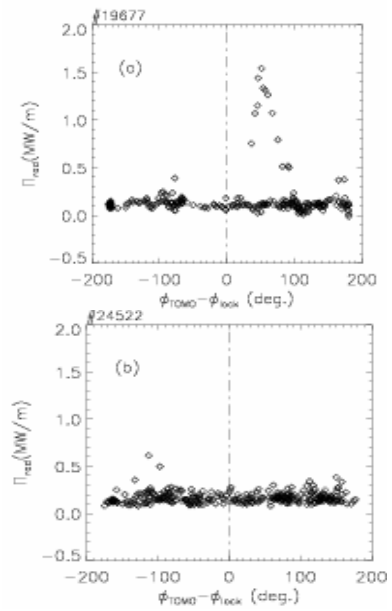

Figure 7) *Total radiated power, integrated over the poloidal section, Π_{rad}, as a function of the angular distance from the locked mode, ϕ_{TOMO}-ϕ_{lock}, in (a) VS and (b) CMC..*

While in CMC there are no signs of toroidally localized regions of increased emissivity, total radiation emissivity maps and multi chord H_α emission diagnostics clearly indicate that plasma wall interaction is poloidally localized and well correlated with the local shift of the last closed magnetic surface. An example is shown in Figure 8. Panel (a) shows the time trace of the horizontal projection of the displacement of the LCMS at the tomographic cross section ($\delta^{(x)}_{,1,-7}(\phi_{TOMO})$) as inferred from magnetic measurements [17]. Positive values represent a displacement in the direction of the low field side. In the panel (a) the radiation asymmetry indicator is also shown. The asymmetry is computed by considering measurements of two vertical bolometric lines of sight passing through regions located on the high and on the low field side: the asymmetry indicator is obtained by normalizing the difference of the two signals to the average. Positive values indicate that radiation is located on the low field side. A clear correlation between the radiation asymmetry and the

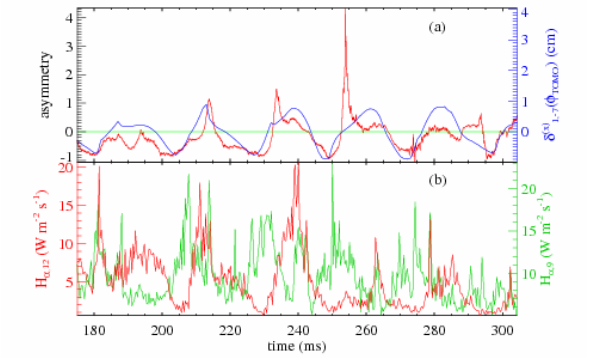

Figure 8) *Helical footprint of the m=1,n=-7 plasma wall interaction in CMC discharges: (a) (blue) local horizontal shift of the plasma surface due to the 1,-7 mode$\delta^{(x)}_{,1,-7}(\phi_{TOMO})$ and (red) bolometric asymmetry indicator; (b) H_α emission from symmetric chords.*

horizontal displacement is observed. Similarly, panel (b) shows H_α emission time traces (measured at a different toroidal angle), as measured by two chords placed opposite with respect to the geometrical section of the vacuum vessel. It appears that the oscillations are out-of-phase and oscillate at the same frequency of the m=1,.n=-7 localized displacement. As both H_α emission and bolometric losses are correlated with plasma wall interaction and they are simultaneously oscillating at the same frequency of the dominant mode, we conclude that the plasma wall interaction is determined by the helical shape of the last closed magnetic surface which is dictated by the m=1,n=-7 periodicity of the dominant TM.

6) Summary

The identification and correction in real time of the aliasing of the sideband harmonics generated by saddle coils led to a significant improvement of the quality of the RFX-mod magnetic boundary as a significant reduction of the last closed magnetic surface is systematically obtained. The adoption of the clean mode control, instead of the virtual shell allows operations with systematic wall unlocking of tearing modes: plasma wall interaction is spread around the first wall during each discharge and it is not toroidally localized as it happened in virtual shell but assumes a distributed helical pattern, rotating at the frequency of the dominant mode. Phase locking between dominant TMs is intermittently partially weakened: indications from transport studies [14] confirm that the reduction of the perturbation amplitudes influences not only the edge but also the plasma core, therefore further optimizations and more accurate modeling of the interaction between the control system and the tearing modes are needed to further improve not only the magnetic boundary but also the overall MHD fluctuations control.

This contract was supported by the Euratom Communities under the contract of Association between Euratom/ENEA. The views and opinions expressed herein do not necessarily reflect those of the European Commission.

[1] CAPPELLO S, et al, Phys. Plas.13 (2006) 056102
[2] ORTOLANI S, SCHNACK DD, *Magnetohydrodynamics of Plasma Relaxation*, (1993) (Singapore: World Scientific)
[3] MARTIN, P. *et al*, Nucl. Fus 43 (2003) 1855
[4] FITZPATRICK R, *et al*, Phys. Plasmas 6 (1999) 3878
[5] PACCAGNELLA R., *et al*., Nucl. Fusion 47 (2007) 990
[6] LUCHETTA A., *et al*., Proc. 21st IAEA Fusion Energy Conference, Chengdu, China (IAEA, Vienna, 2006), vol. IAEA-CN-149, p. FT/P5-1
[7] PACCAGNELLA R., *et al*., Phys. Rev. Lett. 97 (2006) 075001
[8] MARTINI S., *et al*., Nucl. Fus. 47 (2007) 783
[9] ZANCA P., et al. ,Nucl. Fusion, 47 (2007) 1425
[10] MARRELLI L., *et al*., Plasma Phys. Control. Fusion 49 (2007) B359
[11] PACCAGNELLA R, *et al*. Nucl. Fusion 42 (2002)1102
[12] LUCHETTA A, *et al* this conference p. FT/P2-20
[13] TERRANOVA D., *et al*, Plas. Phys. Contr. Fus. 47 (2005) 1047
[14] CARRARO L. *et al*, this conference, p. EX/P3-9
[15] MARRELLI L., *et al*., J. Nucl. Mater. 266-269, 877 (1999)
[16] VALISA M., *et al*., Proc. 21st IAEA Fusion Energy Conference, Chengdu, China (IAEA, Vienna, 2006), vol. IAEA-CN-149, p. EX/P3-17,
[17] ZANCA P., TERRANOVA D., Plasma Phys. Control. Fusion 46, 1115 (2004).